

Research Article

Iontophoretic Delivery of Amino Acids and Amino Acid Derivatives Across the Skin *in Vitro*

Philip G. Green,^{1,2} Robert S. Hinz,¹ Christopher Cullander,¹ Grace Yamane,¹ and Richard H. Guy^{1,3}

Received March 15, 1990; accepted April 11, 1991

The effects of penetrant properties (lipophilicity and charge) and of vehicle pH on the iontophoretically enhanced delivery of amino acids and their N-acetylated derivatives have been examined *in vitro*. The penetrants were nine amino acids (five were zwitterionic, two positively charged, and two negatively charged) and four N-acetylated amino acids, which carry a net negative charge at pH 7.4. Iontophoresis at constant current (0.36 mA/cm²), using Ag/AgCl electrodes, was conducted across freshly excised hairless mouse skin. Iontophoretic flux of the zwitterions was significantly greater than passive transport. Delivery from the anode was greater than from the cathode for all zwitterions. The level of enhancement was inversely proportional to permeant octanol/pH 7.4 buffer distribution coefficient. Cathodal iontophoresis of the negatively charged amino acids and of the N-acetylated derivatives produced degrees of enhancement which were significantly greater than those measured for the "neutral" zwitterions. Furthermore, the enhanced flux reached a steady-state level within a few hours for the negatively charged species, whereas the transport of the zwitterions continued to increase with time. Anodal iontophoresis of histidine and lysine, the two positively charged amino acids studied, induced substantial enhancement which was sensitive to the pH of the delivery vehicle. For example, the flux of histidine from an applied solution at pH 4 (where the amino acid carries a net positive charge) was significantly greater than that from a vehicle at pH 7.4 (where histidine is essentially neutral). The behavior of lysine was more complex and suggested a certain degree of neutralization of the skin's net negative charge.

KEY WORDS: iontophoresis; transdermal drug delivery; amino acid delivery; percutaneous penetration enhancement; skin barrier function.

INTRODUCTION

While iontophoresis has been used to enhance the transdermal flux of many compounds (1), several important issues remain to be resolved (2): (a) the permselectivity of skin, (b) the penetrant structure/properties-enhancement relationships, (c) the paths of ion transport, (d) the degree of tissue damage caused by current flow, and (e) the theoretical basis of iontophoresis. In this work, attention is focused upon initiating a systematic examination of the relationships between penetrant properties (charge, lipophilicity, size, etc.) and iontophoresis enhancement. It is known that, under the driving force of a potential gradient, monovalent cations cross the skin more easily than monovalent anions (3). This permselectivity probably reflects the net negative charge of the skin (4). Furthermore, the preferential flow of cations across the stratum corneum may result in a net volume (electroosmotic) flow of uncharged species in the direction of

positive ion movement (4,5). The influence of external forces, such as vehicle formulation, pH, toxicity, and buffering strength, is also poorly defined.

As our long-term objective is to determine the feasibility of iontophoretically delivering proteins and peptides, this initial investigation has employed as penetrants the "building blocks" of these species, namely, amino acids and their simple derivatives. The effects of permeant charge (neutral versus +1 versus -1), lipophilicity, and vehicle pH have been considered experimentally in an *in vitro* system using excised hairless mouse skin as the model membrane. The following paper (6) addresses how the results reported here compare with those from a series of specially synthesized tripeptides (7).

MATERIALS AND METHODS

Diffusion Cell. Flux measurements were made *in vitro* using a cell (LG 1088-IC, Laboratory Glass Apparatus, Inc., Berkeley, CA) which has been previously described in detail (8). The design of the cell is such that it permits positioning of anode and cathode, in physical and electrical isolation, on the same (stratum corneum) side of a single piece of skin.

¹ Departments of Pharmacy and Pharmaceutical Chemistry, University of California, San Francisco, San Francisco, California 94143.

² Present address: Zyma SA, Nyon 1260, Switzerland.

³ To whom correspondence should be addressed.

This arrangement mimics rather closely, therefore, the configuration of an *in vivo* iontophoretic delivery system. Plastic caps were positioned over the donor chambers of the cells to minimize evaporation of the solutions bathing the electrodes. Small holes were drilled in the caps to allow for electrode insertion and to facilitate the reproducible positioning of the electrodes a fixed distance (~3 mm) from the skin surface.

Electrodes. Ag/AgCl electrodes were preferred over platinum to minimize pH changes in the solutions surrounding the electrodes (due to electrolysis of water) (9). Pure silver wire (1 mm in diameter, 4 cm long, 99.999% pure, from Aldrich Chemical, Co., Milwaukee, WI) was first cleaned with fine emery cloth and one end was manipulated into a small loop. The latter was then coated (10) with silver chloride by dipping the loop into molten AgCl (99.99% pure, from Aldrich Chemical Company, Milwaukee, WI). After cooling, the noncoated Ag wire was protected from contact with the electrolyte by shrink-to-fit, salt-resistant, insulating tubing (1/16-in.-internal diameter, irradiated, flexible polyolefin, from ICO Rally, Palo Alto, CA). The resulting electrodes were robust, durable, and reasonably consistent in surface area. At the end of an experiment, the electrodes were cleaned by gentle sanding with fine emery cloth.

Electrolyte. The receptor phase, perfusing the dermal surface of the skin, and the solutions surrounding anode and cathode in the electrode compartments of the upper half of the cell contained *N*-2-hydroxyethylpiperazine-*N'*-2-ethanesulfonic acid (HEPES)-buffered saline, adjusted to pH 7.4. This electrolyte contained the zwitterionic HEPES buffer at a concentration of 25 mM and the major current-carrying ions, namely, Na⁺ (147 mM) and Cl⁻ (133 mM). This system demonstrates a high buffering capacity at pH 7.4 (3). For the limited experiments involving solutions at pH 4, the HEPES-buffered saline was titrated appropriately with 1

M hydrochloric acid. The resulting solution contained 133 mM Na⁺ and 147 mM Cl⁻.

Skin Source. All experiments used full-thickness skin from female hairless mice (HRS/hr hr, Simonsen Laboratories, Gilroy, CA) that were 8–15 weeks old. The skin was removed from the animals at sacrifice and was used immediately.

Current Delivery. Iontophoresis was performed at constant current (0.36 mA/cm²), supplied to the electrodes from a commercial power supply (Model APH 1000M, Kepco Inc., Flushing, NY), for 18 hr. Throughout each experiment, current and electrode compartment pH were occasionally checked and were found to remain essentially constant.

Permeants. The compounds examined and their radiochemical suppliers are listed in Table I. Iontophoresis was conducted on five zwitterionic ("neutral") amino acids, two positively and two negatively charged amino acids, and four (again, negatively charged) *N*-acetylated amino acid derivatives. The nonradiolabeled permeants were all obtained from Sigma Chemical Co. (St. Louis, MO).

Permeant solutions were freshly prepared before each iontophoretic run by dissolution of the nonradiolabeled chemical in pH 7.4 HEPES-buffered saline to a concentration of 10 mM. The pH of the anionic and cationic permeant solutions was readjusted back to 7.4 by the addition of small volumes of 1 *M* NaOH or 1 *M* HCl, respectively. To enable facile detection and analysis of the permeant in the receptor phase during the course of a diffusion experiment, the permeant solutions were "spiked" with radiolabeled chemical to the extent that each contained approximately 1 μCi/ml.

The purity of the radiochemicals was assessed prior to their use by thin-layer chromatography (TLC). For *N*-acetylvaline and *N*-acetylphenylalanine, it was necessary to use TLC to purify the commercially supplied material. Table II summarizes the TLC conditions and relevant *R_f* values.

Table I. Physicochemical Parameters and Radiochemical Details of the Permeants Studied

Permeant	Molecular weight (da)	log <i>D</i> ^a	p <i>K_a</i> values ^b	Sp. activity (mCi/mMol)	Label position	Supplier ^c
Zwitterions						
Glycine	75.1	-3.11	2.4, 9.8	55	1- ¹⁴ C	ARC
Alanine	89.1	-2.74	2.3, 9.9	135	U- ¹⁴ C	ICN
Valine	117.1	-2.26	2.3, 9.7	225	U- ¹⁴ C	ARC
Leucine	131.2	-1.79	2.3, 9.7	270	U- ¹⁴ C	ICN
Phenylalanine	165.2	-1.43	1.8, 9.2	450	U- ¹⁴ C	ICN
Anions						
Aspartic acid	133.1	-3.47	2.1, 9.8, 4.0	180	U- ¹⁴ C	ICN
Glutamic acid	147.1	-3.40	2.1, 9.7, 4.3	225	U- ¹⁴ C	ICN
Acetylglycine	117.1	-2.99	3.7	55	1- ¹⁴ C	ARC
Acetylalanine	131.1	-2.94	3.7	55	1- ¹⁴ C	ARC
Acetylvaline	159.2	-2.91	3.7	55	1- ¹⁴ C	ARC
Acetylphenylalanine	207.2	-2.77	3.7	55	1- ¹⁴ C	ARC
Cations						
Histidine	155.2	-2.90	1.8, 9.2, 6.0	56.4	2,5- ³ H	NEN
Lysine	146.2	-3.05	2.2, 9.2, 10.8	270	U- ¹⁴ C	ICN

^a *D* = octanol/pH 7.4 HEPES-buffered saline distribution coefficient (11). Histidine value from Ref. 12.

^b Amino acids values from Ref. 13; *N*-acetylated derivatives values from Ref. 14.

^c ARC, American Radiochemicals, Inc., St. Louis, MO; ICN, ICN Radiochemicals, Inc., Irvine, CA; NEN, NEN Research Products, Wilmington, DE.

Table II. Thin-layer Chromatography Details for the Permeants Studied

Permeant	Solvent system	$\sim R_f$
Zwitterions		
Glycine	<i>n</i> -Butanol:acetic acid:water (4:1:5)	0.2
Alanine	<i>n</i> -Butanol:acetic acid:water (4:1:5)	0.2
Valine	Isopropanol:NH ₄ OH (3:1)	0.5
Leucine	<i>n</i> -Butanol:methyl ethyl ketone:water:NH ₄ OH (4:3:2:1)	0.3
Phenylalanine	<i>n</i> -Butanol:ethanol:water (2:2:1)	0.4
Anions		
Aspartic acid	<i>n</i> -Propanol:water (1:1)	0.8
Glutamic acid	<i>n</i> -Propanol:water (1:1)	0.8
Acetylglycine	<i>n</i> -Butanol:acetic acid:water (4:1:5)	0.6
Acetylalanine	<i>n</i> -Butanol:acetic acid:water (4:1:5)	0.7
Acetylvaline	Isopropanol:NH ₄ OH (3:1)	0.7
Acetylphenylalanine	<i>n</i> -Butanol:ethanol:water (2:2:1)	0.7
Cations		
Histidine	<i>n</i> -Propanol:34% NH ₄ OH (7:3)	0.4
Lysine	<i>n</i> -Propanol:34% NH ₄ OH (7:3)	0.2

The TLC procedure used silica gel plates (250- μ m thickness, PE sil G/UV fluorescence, Whatman Ltd., Maidstone, Kent, UK) except in the case of *N*-acetylphenylalanine, which was applied to cellulose (0.1-mm-thickness, plastic-supported, Cellulose F plates, Catalog No. 5504, E. Merck, Darmstadt, West Germany). Retention times for each compound were determined by visualization using ninhydrin spray (Sigma Chemical Co.) for amino acids and *o*-tolidine/Cl₂ (*o*-tolidine in 2% acetic acid (aq.) followed by immersion in a Cl₂ tank) for the *N*-acetylated amino acids.

Iontophoretic Flux Determination. The diffusion cell was assembled with the hairless mouse skin separating the electrode and receptor compartments. The latter was perfused for a 1-hr equilibration period with the pH 7.4 HEPES-buffered saline, which had been degassed prior to use by vacuum filtration through a 0.2- μ m-pore size filter. The electrode compartments of the upper half of the cell were then charged with the appropriate solutions: for the negatively charged permeants, the cathode was immersed in 1 cm³ of the radiolabeled, 10 mM chemical solution, while the anode was surrounded by 1 cm³ of buffered saline; for the positively charged amino acids, the permeant solution was placed in the anode compartment, and the electrolyte surrounded the cathode; for the zwitterions, on separate occasions, both configurations (i.e., delivery from the cathode and delivery from the anode) were studied. The experiment commenced on connection of the electrodes to the power supply. From this point, samples of the continuously perfused receptor phase were collected hourly for 18 hr. The flow rate of 7 cm³/hr was sufficient to exchange the receptor volume completely in a 60-min period. The samples were collected into individual scintillation vials on a preprogrammed fraction collector (Model Retriever III, ISCO Inc., Lincoln, NE). At the end of the experiment, an appropriate volume of scintillation cocktail was added to each vial and the contents were then analyzed for ¹⁴C or ³H by liquid scintillation counting. All iontophoresis experiments were performed a minimum of four times. For each iontophoretic

study, four controls (i.e., following an identical protocol, but with no current) were also carried out. As one hairless mouse yielded sufficient skin for two diffusion cells, each mouse provided a pair of iontophoretic and control data points.

Permeant Octanol/Buffer Distribution Coefficients.

The octanol/pH 7.4 buffer distribution coefficients (*D*) of the zwitterionic and positively charged amino acids were obtained from the literature (11,12). The *D* values of the anionic permeants between 1-octanol (Sigma Chemical Co.) and pH 7.4 HEPES-buffered saline were determined at 20°C. Aqueous electrolyte and octanol were mutually presaturated overnight and then separated. Approximately 0.5 μ Ci of permeant was then added to 0.5 cm³ of electrolyte, which was then equilibrated (with gentle shaking) with 10 cm³ of octanol in a silanized glass culture tube for 24 hr. At the end of this period, the octanol phase was quickly drawn off, without disturbing the lower aqueous layer. The permeant radioactivity in the octanol phase (*R*_o/dpm) was measured by liquid scintillation counting and *D* was then calculated using the following equation:

$$D = \frac{R_o}{R_w^i - R_o} \cdot \frac{V_w}{V_o} \quad (1)$$

where *R*_wⁱ(dpm) is the initial (pre-equilibration) amount of radioactivity in the aqueous electrolyte, and *V*_w and *V*_o are the volumes of electrolyte and octanol, respectively. The *D* values were determined in quadruplicate. The mean values reported in Table I had coefficients of variation of 10% or less.

RESULTS

The passive and iontophoretic fluxes of the zwitterionic amino acids were first compared. Figure 1 illustrates, for alanine, the typical flux profiles observed. Iontophoresis from the anode is significantly more efficient than that from the cathode, and both iontophoretic fluxes are much larger than the passive (no current) control.

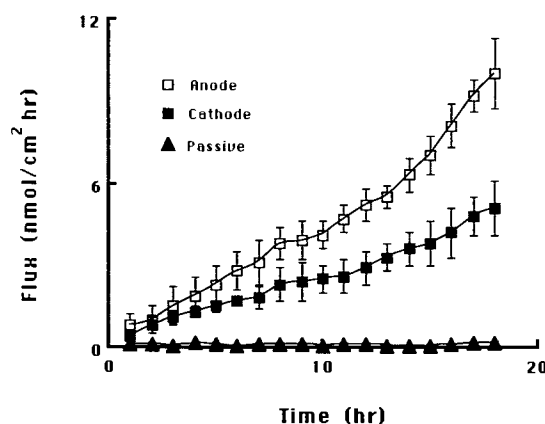


Fig. 1. Flux of alanine, as a function of time, across hairless mouse skin *in vitro* (a) passively (filled triangles), (b) with cathodal iontophoresis (filled squares), and (c) with anodal iontophoresis (open squares). Each data point represents the mean (\pm SD) of four determinations.

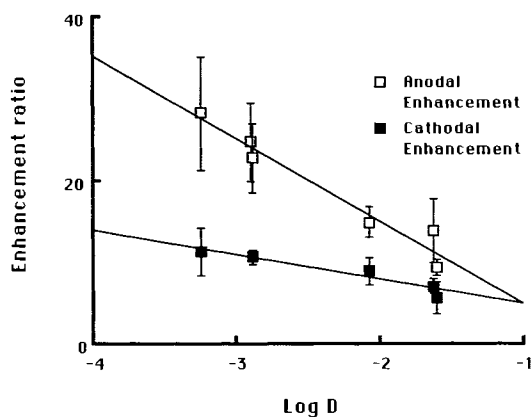


Fig. 2. Anodal (open squares) and cathodal (filled squares) iontophoretic enhancement ratios for five zwitterionic amino acids plotted as a function of octanol/aqueous electrolyte distribution coefficient (D). Each data point represents the mean (\pm SD) of four determinations.

In Fig. 2, the iontophoretic enhancement of the zwitterions for both anodal and cathodal delivery is plotted as a function of the octanol/aqueous electrolyte distribution coefficient. The enhancement ratio (ER) is arbitrarily defined as

$$ER = \frac{\text{cumulative transport with current in 12 hr}}{\text{cumulative passive transport in 12 hr}} \quad (2)$$

As previously noted (16), the ER is greatest for the most hydrophilic penetrants (a fact which also reflects the very low passive permeabilities of these compounds). For anodal iontophoresis, there is a clear inverse proportionality ($r^2 = 0.94$) between ER and $\log D$. For cathodal delivery, however, the relationship is much less apparent.

Under the conditions of the experimental protocol used, it was not possible to detect any passive transport of the anionic permeants studied. In other words, during the 18 hr of the control permeation experiment, the level of radioactivity in the receptor phase did not exceed background counts. The observation confirms, of course, the extreme resistance of the stratum corneum to the movement of charged substances. With cathodal iontophoresis, on the other hand, appreciable flux occurred. A typical profile, as a function of time, for *N*-acetylalanine, is shown in Fig. 3. The flux increases quickly from zero to attain an essentially steady-state level within 3–4 hr. The result (which was characteristic of *all* the negatively charged permeants) is distinctly different from those for the zwitterions. A simple calculation (3) indicates that the transport number of the anions in these experiments is ~ 0.002 .

Figure 4 plots the enhanced cathodal flux of the anionic permeants against the corresponding $\log D$ values. Although the span of $\log D$ is small, there is no perceptible dependence of flux on lipophilicity in this case.

During the course of the iontophoresis experiment, it is possible that either (a) electrolytic degradation or (b) in the case of the *N*-acetylated derivatives, hydrolysis of the permeants may occur. To check for these eventualities, using *N*-acetylalanine as a model compound, the receptor phase

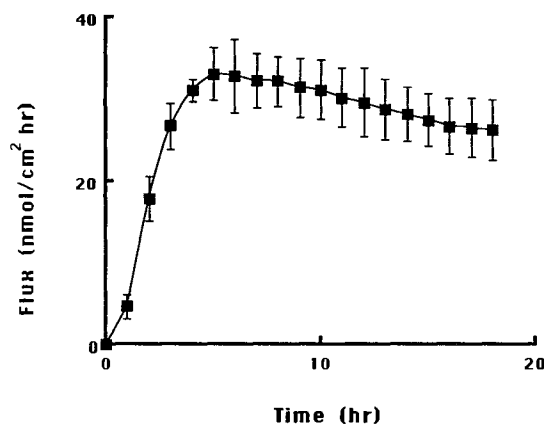


Fig. 3. Flux of acetylalanine, as a function of time, with cathodal iontophoresis. Each data point is the mean (\pm SD) of four determinations.

fractions were combined and freeze-dried. Subsequently, the lyophilized sample was partially reconstituted in ethanol and was then examined (after centrifugation and decanting of the supernatant) by TLC. The solvent used for the chromatography is given in Table II. Because of the high salt concentration in the lyophilized powder, a two-phase silica gel plate (250- μ m thickness, LK 5 DF, linear K silica gel, Whatman, Maidstone, Kent, UK) was employed. It was found that $91.1 \pm 4.9\%$ ($n = 3$) of the radioactivity in the combined receptor phase samples had an R_f value identical to that of the pure *N*-acetylalanine. The corresponding procedure carried out on triplicate samples of the donor phase at $t = 0$ hr (i.e., before iontophoresis) and $t = 18$ hr (at the end of the experiment) showed that 95.2 ± 3.3 and $94.7 \pm 4.1\%$, respectively, of the radioactivity was the intact derivative. In large part, therefore, no degradation of the permeant could be detected.

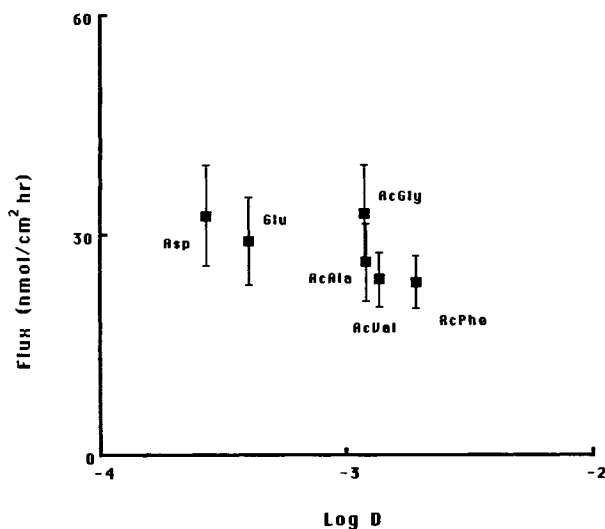


Fig. 4. Steady-state fluxes of six anionic permeants following cathodal iontophoresis plotted as a function of octanol/aqueous electrolyte distribution coefficient (D). Each data point is the mean (\pm SD) of four determinations.

The (positively) ionizable amino acids, histidine and lysine, were chosen to initiate examination of the effect of permeant charge on iontophoretic enhancement. To do so, the ER values of the two compounds were assessed at two different donor solution pHs (see Fig. 5). The pK_a values of histidine are 1.8, 6.0 and 9.2. Hence, at pH 7.4, the amino acid is essentially uncharged, whereas at pH 4, it carries a net positive (+1) charge. The histidine donor solutions surrounded, of course, the anode, and as expected, a significant promotion of transdermal flux was observed as the penetrant assumed a positive charge (i.e., as the pH was changed from 7.4 to 4). The ER at pH 7.4 is quite consistent (with respect to the $\log D$ of histidine) with the zwitterionic data reported above (see Fig. 2). For comparison with the anionic permeant results, the histidine flux after 12 hr of iontophoresis from a pH 4 donor solution was approximately 100 (± 12) nmol/cm²/hr. In other words, iontophoretic enhancement of this cation was significantly greater than that of the anions studied. The pK_a values of lysine are 2.2, 9.2, and 10.8. Hence, lysine carries a net positive (+1) charge at both pH 7.4 and pH 4. Now, however, in addition to the large ER values *per se*, we observe, unexpectedly, that the ER is smaller at the lower pH.

DISCUSSION

To understand the iontophoretic flux data presented in this paper, transport of all ions present in the diffusion cell must be considered (16). In particular, because the anodal and cathodal chambers were of finite volume, and because no replenishment of solution in these chambers was performed during the 18-hr time course of the experiment, significant changes in the identity of the current-carrying species can be expected.

Consider first the anodal iontophoresis of positively charged lysine at pH 7.4. From Faraday's law, the flux of lysine (J_{L^+}) at time T in an applied electric field is

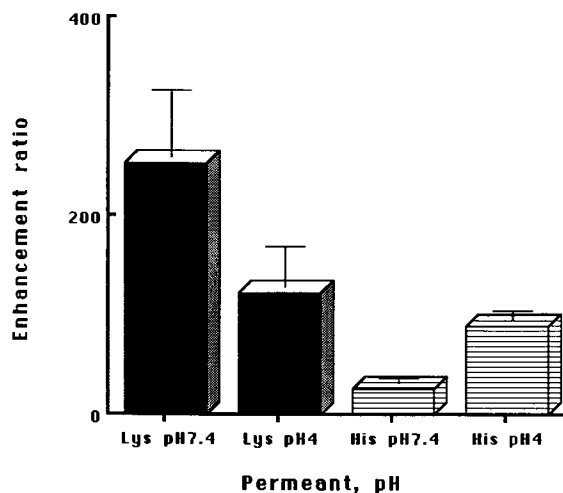


Fig. 5. Anodal iontophoretic enhancement ratios (mean \pm SD; $n = 4$) of lysine (Lys) and histidine (His) determined at pH 4 and at pH 7.4.

$$J_{L^+}^T = \frac{t_{L^+}^T \cdot I_D}{Z_{L^+} \cdot F} \quad (3)$$

$$= \frac{Z_{L^+} \cdot U_{L^+} \cdot C_{L^+}^T}{\sum_{i=1}^n Z_i \cdot U_i \cdot C_i^T} \cdot \left(\frac{I_D}{Z_{L^+} \cdot F} \right) \quad (4)$$

$$= \frac{I_D \cdot U_{L^+} \cdot C_{L^+}^T}{F \sum_{i=1}^n Z_i \cdot U_i \cdot C_i^T}$$

where $t_{L^+}^T$ and $C_{L^+}^T$ are the transport number and concentration, respectively, of lysine at time T , Z_{L^+} is the charge of the lysine anion (+1), I_D is the current density, F is Faraday's constant, U_{L^+} is the mobility of the lysine anion, and

$$\sum_{i=1}^n Z_i \cdot U_i \cdot C_i^T$$

is the summation of the (charge) \times (mobility) \times (concentration at time T) product for the other ions in the system.

Note that Eq. (4) predicts that J_{L^+} depends upon the mole fraction of lysine present in the donor chamber, and not on its absolute concentration (17). Now, in the experiments reported here, the other principal ions present are Na^+ and Cl^- . It follows that Eq. (4) can be rewritten:

$$J_{L^+}^T = \frac{\{I_D \cdot U_{L^+} \cdot C_{L^+}^T\}}{F \cdot [U_{Na^+} \cdot C_{Na^+}^T + U_{Cl^-} \cdot C_{Cl^-} + U_{L^+} \cdot C_{L^+}^T]} \quad (5)$$

where the relevant chloride ion concentration (C_{Cl^-}), of course, is that in the perfusing receptor solution beneath the skin. Equation (5) assumes that, throughout the experiment, (i) ionic mobilities are constant, (ii) C_{Cl^-} in the receptor compartment does not differ significantly from the perfusing solution concentration (0.133 M), and (iii) no interactions occur between ions within the skin. We further assume, following Burnette and Ongpipattanakul (2,3), that (a) $t_{Na^+} > t_{Cl^-}$, (b) $t_{Na^+}/t_{Cl^-} \approx 2.5$, and (c) $t_{Na^+}, t_{Cl^-} \gg t_{L^+}$. Consequently, $U_{Na^+} \cdot C_{Na^+} \gg U_{L^+} \cdot C_{L^+} \ll U_{Cl^-} \cdot C_{Cl^-}$, and Eq. (5) reduces to

$$J_{L^+}^T = \frac{\{I_D \cdot U_{L^+} \cdot C_{L^+}^T\}}{F \cdot [U_{Na^+} \cdot C_{Na^+}^T + U_{Cl^-} \cdot C_{Cl^-}]} \quad (6)$$

It can be deduced immediately that $J_{L^+}^T$ is going to be sensitive to the temporal changes occurring in $C_{L^+}^T$ and $C_{Na^+}^T$. The experimental data show that C_{L^+} changes by only a very small amount over 18 hr (confirming that $t_{L^+} \ll t_{Na^+}$); however, as we now demonstrate, C_{Na^+} decreases appreciably during the iontophoresis, thereby allowing $J_{L^+}^T$ to increase with time.

We define the following ratio (R_{L^+}):

$$R_{L^+} = \frac{J_{L^+}^T}{J_{L^+}^6} \quad (7)$$

where $J_{L^+}^6$ is the lysine flux 6 hr after the initiation of iontophoresis. From Eq. (6), given that $C_{L^+}^6 \approx C_{L^+}^T$ and that $C_{Cl^-} = 0.133 M$, it follows that

$$R_{L^+} = \frac{\{U_{Na^+} \cdot C_{Na^+}^6 + 0.133 \cdot U_{Cl^-}\}}{[U_{Na^+} \cdot C_{Na^+}^T + 0.133 \cdot U_{Cl^-}]} \quad (8)$$

The apparently arbitrary choice of $T = 6$ hr is based upon the availability of concentration, mobility, and transport number data for Na^+ and Cl^- under similar conditions from the work of Burnette and Ongpipattanakul (3). They showed that at $T = 6$ hr, $t_{Na^+}/t_{Cl^-} \approx 2.5$, from their data, we calculate $C_{Na^+}^6 = 0.137 M$, and we know that $C_{Cl^-}^6 = 0.133 M$; hence, $U_{Na^+}/U_{Cl^-} \approx 2.4$, and Eq. (8) reduces to

$$R_{L^+} = \frac{(C_{Na^+}^6 + 0.0554)}{(C_{Na^+}^T + 0.0554)} \quad (9)$$

Furthermore, at steady state, at 0.36 mA/cm^2 , data from these same authors predict that $J_{Na^+} \approx 8 \text{ mmol/cm}^2/\text{hr}$, which translates to about 4.4 mmol/hr in our cells ($A = 0.55 \text{ cm}^2$). Thus, in 18 hr, we estimate that the Na^+ concentration in the anodal chamber could have decreased by as much as 54%.

Now consider briefly the cathodal iontophoresis of a negatively charged permeant (e.g., acetylalanine, AA^-). In this case, it is the chloride ion concentration in the donor chamber that changes, while the Na^+ level in the perfusing receptor compartment remains fixed (at $0.147 M$). The equivalent expression to Eq. (8) is, therefore,

$$R_{AA^-} = \frac{J_{AA^-}^T}{J_{AA^-}^6} = \frac{\{0.147 \cdot U_{Na^+} + U_{Cl^-} \cdot C_{Cl^-}^6\}}{[0.147 \cdot U_{Na^+} + U_{Cl^-} \cdot C_{Cl^-}^T]} \quad (10)$$

Again, from the literature (3), $U_{Na^+}/U_{Cl^-} = 2.4$, and hence

$$R_{AA^-} = \frac{(0.353 + C_{Cl^-}^6)}{(0.353 + C_{Cl^-}^T)} \quad (11)$$

Although one might at first expect $C_{Cl^-}^T$ to decrease (and, hence, R_{AA^-} to increase) with time, this is not the case. The Cl^- concentration in the donor chamber changes in two ways: (i) it depletes because Cl^- is subject to an electrorepulsive force from the cathode which drives ions into the skin, and (ii) it increases because of the electrode reaction: $AgCl(s) + \bar{e} \rightarrow Ag^0(s) + Cl^-(aq)$, which must occur to provide counterions for the Na^+ species which are being attracted from and beneath the skin to the negatively charged cathode. Because of skin permselectivity, the creation of $Cl^-(aq)$ from the electrode exceeds the electrorepulsive depletion by an amount equal to the net movement of Na^+ (as calculated above). Consequently, C_{Cl^-} in the cathode chamber actually increases with time of iontophoresis, and a decrease in acetylalanine flux is therefore anticipated.

The predictions of Eqs. (9) and (11) can now be compared with the experimental data. First, we examine lysine flux from the pH 7.4 donor solution. The values calculated for R_{L^+} using Eq. (9) are presented with the iontophoretic measurements of the same quantity in Table III. Qualitatively, the model predicts the observed pattern of behavior well, and the lysine flux increases progressively with increasing time, as the Na^+ concentration decreases. Quantitatively, though, the agreement is less good and the deviation between theory and experiment becomes greater as the time of iontophoresis is prolonged. Coincidence between

Table III. Experimental Measurements, and Theoretical Predictions [Using Eq. (9)], of R_{L^+} for Lysine Iontophoresis at pH 7.4^a

Time (hr)	R_{L^+} (experiment)	R_{L^+} (theory)	Difference ^b
6	1.00	1.00	0.00
7	1.04	1.03	+0.01
8	1.08	1.06	+0.02
9	1.28	1.09	+0.19
10	1.41	1.12	+0.29
12	1.64	1.18	+0.46
14	1.92	1.26	+0.66
16	2.04	1.35	+0.69
18	2.25	1.44	+0.81

^a The lysine iontophoretic flux at 6 hr was $62.5 \text{ nmol cm}^{-2} \text{ hr}^{-1}$; passive transport was not detectable during the 18-hr run.

^b R_{L^+} (experiment) - R_{L^+} (theory).

theory and experiment is better for the cathodal delivery of acetylalanine (Table IV). The anionic flux decreases with increasing time as explained above.

While the pH dependence of histidine flux (Fig. 5) is expected, the reason for lysine to penetrate more poorly at pH 4 than at pH 7.4 is not intuitively obvious. However, recalling that permselectivity (2) indicates that the membrane supports a net negative charge, one explanation for this result is that, at lower pH, there is some neutralization of this negativity, thereby undermining the "power" of the penetrant's +1 charge. Further experiments are necessary to explain fully the results in Fig. 5. Parenthetically, one might add that there have been previous reports of apparently inconsistent findings when positively chargeable permeant flux has been determined as a function of pH [e.g., the results of Burnette and Marrero (4) using thyrotropin releasing hormone]. Because the alteration of pH can result in multiple changes other than the ionization state of the permeant (such as the distribution and identity of charge carriers, the net charge on the membrane, etc.), interpretation of these experiments is complex. Second, the transport results for the negatively charged penetrants support an often-cited advantage of iontophoresis, namely, that the procedure can permit enhanced and reproducible drug delivery across a notoriously variable membrane (i.e., the skin) (18). In the case of anionic transport, despite the changes in ionic con-

Table IV. Experimental Measurements, and Theoretical Predictions [Using Eq. (11)], of R_{AA^-} for Acetylalanine Iontophoresis (Fig. 3)

Time (hr)	R_{AA^-} (experiment)	R_{AA^-} (theory)	Difference ^a
6	1.00	1.00	0.00
7	0.99	0.99	0.01
8	0.99	0.98	+0.01
9	0.96	0.97	-0.01
10	0.94	0.97	-0.03
12	0.91	0.95	-0.04
14	0.86	0.94	-0.08
16	0.82	0.92	-0.10
18	0.82	0.91	-0.09

^a R_{AA^-} (experiment) - R_{AA^-} (theory).

centrations in the donor chamber, the flux of penetrant remains relatively constant because of the reservoir of Na⁺ beneath the skin (an *in vivo* feature mimicked by the diffusion cell design). Precise control of transport by the value of applied current is anticipated, therefore.

Finally, we turn to zwitterionic amino acids (Figs. 1 and 2). The greater enhancement induced by anodal delivery is probably related to the permselectivity of the skin: the major current-carrying positive ion in the zwitterion experiments is Na⁺; chloride is the principal current-carrying anion, the transport number of which is approximately one-half that of Na⁺ (3). The flow of these ions across the skin causes an electroosmotic water flow, which has been defined (2) as the net flow of solvent induced by the momentum transfer from the movement of charged species under an applied potential difference. In addition, because of the reversible nature of the Ag/AgCl electrodes used, and because the HEPES-buffered saline electrolyte is present in all chambers of the diffusion cell, current flow leads to the net movement of salt ions from the solution surrounding the anode to that surrounding the cathode. This induced concentration gradient then causes an osmotic flow of water from anode to cathode. Thus, a complex pattern of convective solvent flow is caused by current passage, apparently with preferential effect away from the anode. However, Fig. 1 indicates that the situation is even more complicated. The flux of zwitterions under the imposition of a potential difference does not attain a steady state within 18 hr, despite the large reservoir of permeant available in the donor chamber and the effectively "sink" conditions maintained in the receptor phase. In fact, the flux continues to increase with increasing time of iontophoresis.

The pattern of behavior seen here (increasing flux of an effectively neutral species with increasing time of iontophoresis) has also been observed for other permeants, including mannitol (3), glycine, glucose, and tyrosine (19). While the explanation of these findings is not straightforward, a number of hypotheses may be advanced. (a) The permeants bind to specific sites located in the transport pathways through the skin (20). While this would not be expected to alter the steady-state flux level, it would prolong the time necessary to attain steady state. (b) Along similar lines of reasoning, the uptake of polar permeants into the skin may lead to a progressively favorable partitioning environment for these molecules, with the result that transport continually increases with time. (c) There may be changes induced in the skin by the passage of current which leads to a time-dependent change in barrier properties, manifested by easier access to polar permeant penetration. This may include changes in hydration level, which, because of the convective flow of water, may reduce barrier function more quickly than observed in passive permeation experiments (21), or differential effects on the various putative pathways that have been inferred from previous investigations (2,16,17,22). Further deductions about the exact nature of the structural/physical changes taking place await additional measurements and/or direct visualization of the tissue either during or immediately after current passage.

In summary, the results presented in this paper show that iontophoresis can cause significant augmentation of amino acid transport across the skin. Delivery of charged amino acids, or their derivatives, is reasonably well ex-

plained by considering the flow of all ions in the system. The iontophoretic flux of zwitterionic (i.e., essentially neutral) species does not attain steady state under the conditions of the experiments performed. While a number of reasons for this behavior can be advanced, the precise explanation remains, at this time, unknown.

ACKNOWLEDGMENTS

This research was supported by grants from the National Institutes of Health (HD-27839), Cygnus Therapeutic Systems, and Hoffmann-LaRoche. We thank Peter Juhasz of LGA, Berkeley, CA, for his continuing efforts to develop our diffusion cell design and Andrea Mazel for assistance with manuscript preparation. Helpful comments and suggestions were contributed by Peretz Glikfeld, Girish Rao, and Professors Ron Burnette and John Albery.

REFERENCES

1. P. Tyle. Iontophoretic devices for drug delivery. *Pharm. Res.* 3:318-326 (1986).
2. R. R. Burnette. Iontophoresis. In J. Hadgraft and R. H. Guy (eds.), *Transdermal Drug Delivery. Developmental Issues and Research Initiatives*, Marcel Dekker, New York, 1989, pp. 247-291.
3. R. R. Burnette and B. Ongpipattanakul. Characterization of the permselective properties of excised human skin during iontophoresis. *J. Pharm. Sci.* 76:765-773 (1987).
4. R. R. Burnette and D. Marrero. Comparison between the iontophoretic and passive transport of thyrotropin. *J. Pharm. Sci.* 75:738-743 (1986).
5. L. P. Gangarosa, N. H. Park, C. A. Wiggins, and J. M. Hill. Increased penetration of nonelectrolytes into mouse skin during iontophoretic water transport (iontohydrokinesis). *J. Pharm. Exp. Ther.* 212:377-381 (1980).
6. P. G. Green, R. S. Hinz, A. Kim, F. Szoka, and R. H. Guy. Iontophoretic delivery of a series of tripeptides across the skin *in vitro*. *Pharm. Res.* 8:1121-1127 (1991).
7. A. Kim and F. Szoka. The distribution of tripeptides between octanol and water (submitted for publication).
8. P. Glikfeld, C. Cullander, R. S. Hinz, and R. H. Guy. A new system for *in vitro* studies of iontophoresis. *Pharm. Res.* 5:443-446 (1988).
9. D. R. Crow. *Principles and Applications of Electrochemistry*, 2nd ed., Chapman and Hall, London, 1979.
10. R. C. Thomas, *Ion-Selective Intracellular Microelectrodes: How to Make and Use Them*, Academic Press, London, 1978.
11. L. M. Yungler and R. D. Cramer. Measurement and correlation of partition coefficients of polar amino acids. *Mol. Pharmacol.* 20:602-608 (1981).
12. J. L. Fauchere and V. Pliska. Hydrophobic parameters P of amino-acid side chains from the partitioning of N-acetyl-amino-acid amides. *Eur. J. Med. Chem. Chim. Ther.* 18:369-375 (1983).
13. *Handbook of Chemistry and Physics*, 66th ed., CRC Press, Boca Raton, Fla., 1985.
14. G. Kortüm, W. Vogel, and K. Andrusson. *I.U.P.A.C. Dissociation Constants of Acids in Aqueous Solution*, Butterworth, London, 1961.
15. S. Del Terzo, C. R. Behl, and A. R. Nash. Iontophoretic transport of a homologous series of ionized and nonionized model compounds: Influence of hydrophobicity and mechanistic interpretation. *Pharm. Res.* 6:85-90 (1989).
16. M. J. Pikal and S. Shah. Transport mechanisms in iontophoresis. II. Electroosmotic flow and transference number measurements for hairless mouse skin. *Pharm. Res.* 7:213-221 (1990).
17. J. B. Phipps, J. M. Sunram, and R. V. Padmanabhan. The ef-

- fect of extraneous ions on the transdermal iontophoretic delivery of hydromorphone. *Proc. Int. Symp. Control. Rel. Bioact. Mater.* 16:50-51 (1989).
18. B. W. Barry. *Dermatological Formulations—Percutaneous Absorption*. Marcel Dekker, New York, 1983, p. 236.
 19. M. J. Pikal and S. Shah. Transport mechanisms in iontophoresis. III. An experimental study of the contributions of electroosmotic flow and permeability change in the transport of low and high molecular weight solutes. *Pharm. Res.* 7:222-229 (1990).
 20. L. L. Wearley, K. Tojo, and Y. W. Chien. A numerical approach to study the effect of binding on the iontophoretic rate of transport of a series of amino acids. *J. Pharm. Sci.* 79:992-998 (1990).
 21. R. S. Hinz, C. D. Hodson, C. R. Lorence, and R. H. Guy. *In vitro* percutaneous penetration: Evaluation of the utility of hairless mouse skin. *J. Invest. Dermatol.* 93:87-92 (1989).
 22. M. J. Pikal. Transport mechanisms in iontophoresis. I. A theoretical model for the effect of electroosmotic flow on flux enhancement in transdermal iontophoresis. *Pharm. Res.* 7:118-126 (1990).